Muscle fiber hyperplasia and its relation to muscle growth

Master thesis in Molecular Biosciences

Main field of study in Physiology

Grant Bullock

60 study points

Section for Physiology and Cell Biology

Department of Biosciences

The faculty of Mathematics and Natural Sciences

University of Oslo

2015

Acknowledgements

The work presented in this thesis was performed at the Program for Physiology and Cell Biology, Department of Biosciences.

The work presented in this thesis was performed at the Program for Physiology and Cell biology, Department of Biosciences, University of Oslo, between September 2014 and June 2015, under the supervision of Professor Kristian Gundersen.

As a foreigner in a foreign land, I found the welcoming of the Gundersen group extremely warm. You all have been paramount to the completion of my project and an enormous source of support both academically and emotionally. I would also like to thank the tax-payers of Norway for supporting my scientific endeavors.

Kristian Gundersen, I would like to thank you for affording me the opportunity to be a part of your research group, it was a tremendous opportunity and experience of which I will be forever grateful. I would like to thank you for your tutelage, and support throughout my academic career with the University of Oslo. Professor Gundersen, you encouraged my independence while correcting my heading when I strayed off course.

Jo C. Bruusgaard I thank you for always making time for me, and for always being source of help when I needed it. Ingrid Marie Egner I thank you for always finding a polite way of allowing me to pretend that I did in fact understand my work. Ingrid you kept me strong, laughing, and forever understanding the struggle of Brenda's whole society, for this I thank you. Ivan Myhre Winje, I thank you for being my friend and for showing me that world class scientific research and fun are not mutually exclusive. Einar Eftestøl, I thank you for being a voice of reason, for giving me the critiques I didn't want to hear but that I needed. Margrethe I thank you for putting up with me talking about random nonsense in the study room, and for listening. Tine Norman Alver, I thank you for being my science Sherpa, and showing me the ropes of the Gundersen lab. I would like to thank Hilde and Gunnar in the animal facility for all the help and advice. To all the members of the Physiology department, I thank you for providing a professional and social environment. Til slutt vil jeg takke kjæresten min Yvonne, for å sette opp med meg ikke dusjing de siste ukene mens jeg ferdig med denne oppgaven.

Abstract

It has long been understood that an increased work load, or demand, will cause an increase in muscle size. As a muscle adds mass, it must either increase the size of individual muscle fibers (hypertrophy), or increase the number of muscle fibers (hyperplasia). Today, most of the evidence supports hypertrophy as the main mechanism behind muscle growth. The role of hyperplasia in this process is not well understood. The existence of bifurcated muscle fibers in adult samples has been observed, but there is contention surrounding their purpose and prevalence. Evidence of adult fiber splitting has been recorded in many animals, although most of the evidence comes from bird studies, and very little from mammals.

To better understand this phenomenon, we investigated the existence of hyperplasia after overload via synergist ablation. Four groups of mice were subject to surgical synergistic ablation to induce overload. The *tibialis anterior* (TA) muscle was removed from the left hind limb in order to create an increased load on the *extensor digitorum longus* (EDL) muscle. Mice were then sacrificed at two weeks, three weeks, four weeks, and five weeks post ablation. EDL muscles were either removed and frozen for sectioning and subsequent staining, or they were removed and macerated for fiber teasing and subsequent visualization under light microscopy.

Using various staining and labeling techniques, we were unable to show evidence of significant muscle fiber hyperplasia. In the highest incidence group, five weeks post overload, split fibers only made up 3.6% of the total fiber number. Differential staining of collagen and dystrophin revealed possible split fibers in 4 of 24 muscle samples. Considering our very low incidence of split fibers, it stands to reason that fiber splitting has a very small impact on total muscle growth and force as compared to the observed hypertrophy of existing fibers. Hypertrophy remains as the most and possibly only mechanism of increasing size and force in adult muscle.

These results suggest that although skeletal muscle hyperplasia might occur in adult mice, it occurs at a very low level.

Table of contents

Acknowledgements **3**

Abstract **5**

1 Introduction **9**

1.1 Skeletal muscle growth and the myonuclear domain 9

1.1.1 The avian model of muscle growth 10

1.1.2 Marine Models of muscle growth 11

1.1.3. Experimental models of muscle growth in mammals 13

1.2 Aims of study 15

2. Materials and Methods **16**

2.1 Experiments on animals and tissues 16

2.1.1 Animals 16

2.1.2 Surgical procedures 16

2.1.3 Synergist Ablations 16

2.1.4 In vivo transfection/Electroporation 17

2.1.5 Maceration 18

2.1.6 Fiber teasing 18

2.1.7 Perfusion 18

2.1.8 Measurements of cross sectional area 19

2.1.9 Analysis of collagen and dystrophin dissimilarities 20

2.2 Histology 21

2.2.1 Removal of muscles 21

2.2.2 Snap-freezing of muscles 21

2.2.3 Cryo-sectioning 21

2.2.4 Staining with haemotoxylin 21

2.2.5 Staining with hoechst 22

2.2.6 Staining for laminin 22

2.2.7 Staining for phalloidin 23

2.2.8 Staining for Collagen and dystrophin 23

2.3.9 Fluorescent microscopy 23

2.3.10 Confocal microscopy 23

2.4 Statistical procedures 24

3 Results **25**

3.1 Measurement of cross sectional area 25

3.2 Frequency distribution of fiber cross sectional area 27

3.3 Maceration and Fiber teasing 28
3.4 Electroporation and plasmid transformation 30
3.5 Collagen and dystrophin staining 31

4 Discussion 32
4.1 Muscle overload results in a very low level of fibers with a split appearance 32
4.2 Explanation to the observed fiber bifurcation 33
4.3 Possible regeneration 34
4.4 Unsuccessful Experiments 35
4.5 Future directions and applications 36
4.6 Conclusion 37

5 References 38

6 Appendix 44
6.1 List of abbreviations 44
6.2 Buffers and solutions 44
6.2.1 10X PBS (phosphate buffered saline) solution 44
6.2.2 Hoechst solution 45
6.2.3 ZRF cocktail solution 45
6.2.4 Permeabilization buffer 45
6.2.5 DNA electroporation solutions 45
6.3 Histochemistry 46
6.3.1 Staining for laminin 46
6.3.2 Staining for collagen 46
6.3.3 Staining for dystrophin 47
6.3.3 Staining for phalloidin 47

1 Introduction

1.1 Skeletal muscle growth and the myonuclear domain

The fundamental unit of the muscle is a contractile unit known as the sarcomere. Any physiology textbook will tell you that all force in the muscle cell ultimately comes from the number of sarcomeres available. It is well understood that a muscle subjected to increasing load will compensate and become stronger by means of an increase in its contractile tissue, fiber size and protein synthesis (Adams, 1997; Booth, Tseng, Flück, & Carson, 1998; Rennie, Wackerhage, Spangenburg, & Booth, 2004; Tipton & Wolfe, 1998). The muscle fiber is special in that it is one of the few multinucleated cells of the human body. Within the muscle fiber, each nucleus will synthesize protein for a specific domain in the vicinity of that specific nucleus. This characteristic of each nucleus having its own domain, is known as the myonuclear domain (MND) (Hall & Ralston, 1989; Pavlath, Rich, Webster, & Blau, 1989)

As a muscle fiber grows in size, one would expect the myonuclear domain to increase, as each myonuclei must now cater to the synthetic needs of a larger volume. However this does not seem to be the case, new myonuclei are recruited to the growing fiber to maintain a normal myonuclear domain (Bruusgaard, Johansen, Egner, Rana, & Gundersen, 2010). Myonuclei are not evenly spaced about the muscle cell, they are located around the periphery (Shenkman, Turtikova, Nemirovskaya, & Grigoriev, 2010). Even with an increase in myonuclei, as a muscle grows, the myonuclei must cover a larger distance to transport and receive from the center of the cell. There exists a point at which the myonuclear domain can become too large to efficiently service its synthetic and metabolic needs (Gallanti et al., 1992; Kadi et al., 2004).

Faced with the problem of increasing myonuclear domains, the muscle fiber has 3 options, it can increase synthetic output of existing nuclei, it can recruit nuclei, or it can decrease its fiber area by splitting. An increased myonuclear domain has been shown to increase protein synthesis via the PI3K/AKT pathway mediated by mTor (Egerman & Glass, 2014). Myonuclear recruitment has also been shown to occur following training and prior to muscle hypertrophy, resulting in an increased number of myonuclei (Bruusgaard et al., 2010). Given their peripheral location, an increase in myonuclei will still be met with a transport problem, as the fiber gets increasingly large. Therefore, it follows logically, that to decrease the myonuclear domain, and thus maintain an efficient nuclear transport and diffusion distance; the fiber could increase its myonuclear count, as well as decrease its volume and split into two. The idea of skeletal muscle fiber hyperplasia is a poorly understood and often contended notion.

Embryonic myogenesis is the process by which developing organisms produce muscle tissue from embryonic somites. Embryogenesis resembles muscle fiber repair and regeneration and not so much growth (Zhao & Hoffman, 2004). The scientific canon asserts that the process of increasing muscle tissue in the adult mammal is markedly different than myogenesis and has been shown to involve the growth of individual cells in the form of hypertrophy more so than the recruitment and development of new cells. Recently however, the idea has been challenged that hypertrophy alone is the driving force behind an increase in muscle growth and not hyperplasia.

There is doubt surrounding the very existence of skeletal muscle hyperplasia in adults, and whether hypertrophy of existing muscle fibers entirely determines muscle enlargement (McCall, Byrnes, Dickinson, Pattany, & Fleck, 1996). There have been various reports of fiber splitting, or bifurcated fibers in athletic humans. In fact, split fibers are often seen in high level power athletes, as well as weight lifting animals (Gallanti et al., 1992). Many studies have been performed to examine the nature of skeletal muscle fiber splitting, and unfortunately, the results vary greatly. Some results support the idea of skeletal fiber hyperplasia (Gallanti et al., 1992; Larsson & Tesch, 1986; Tesch, 1988) (Gonyea, 1980; Gonyea, Sale, Gonyea, & Mikesky, 1986; Tamaki, Uchiyama, & Nakano, 1992; Vaughan & Goldspink, 1979), and some refute it outright (Gollnick, Timson, Moore, & Riedy, 1981; McCall et al., 1996; Schmalbruch, 1976; Sjostrom, Lexell, Eriksson, & Taylor, 1991), while some manage to support and refute the idea within the same sample (MacDougall, Sale, Alway, & Sutton, 1984; MacDougall, Sale, Elder, & Sutton, 1982). Although there is a poor depth of knowledge regarding skeletal muscle fiber hyperplasia in adult mammals, other animal models have shown promising results.

1.1.1 The avian model of muscle growth

The avian model of overload has been shown to produce larger increases in skeletal muscle hyperplasia than seen in mammalian models (Kelley, 1996). Stretch is a common method of overloading the muscle and has been shown to cause an increase in fiber number. Quail ALD (Anterior Latissimus Dorsi) were subjected to progressive stretch overload (PSO) via hanging weights attached to the wing of the quail. After a period of 30 days, there was a 172% increase in muscle mass with a 52% increase in fiber number (Figure 1). 60 days post removal of weighted stretch apparatus, there was still a 41% increase in fiber number, yet fiber cross sectional area had returned to control levels (Antonio & Gonyea, 1993). It is suggested that as the fiber area increased, its myonuclear domain reached a maximum and the fibers split to mediate this stress.

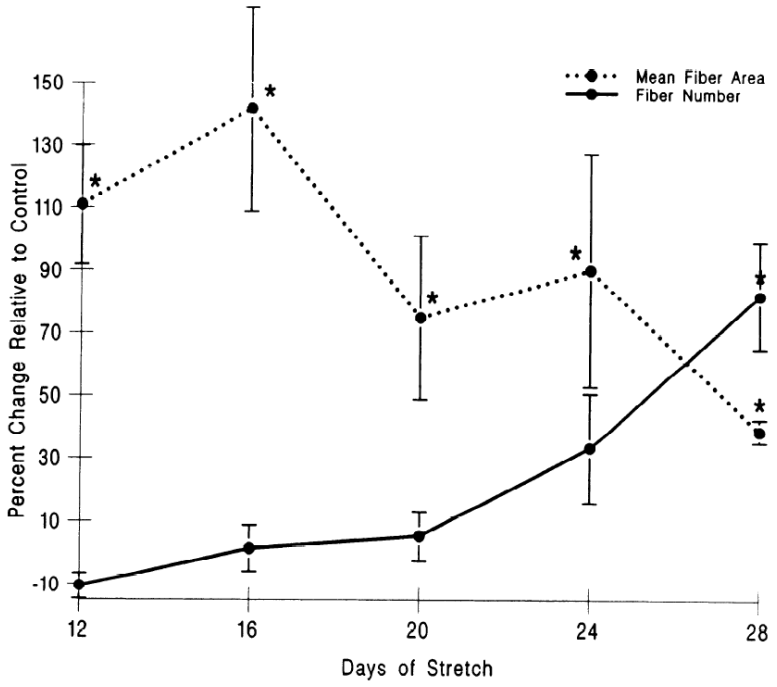

Figure 1. Progressive stretch overload of the quail ALD (Antonio & Gonyea, 1993)
Increasing amount of weights is attached to a collar around the wing of a quail to induce stretch and subsequent muscle growth. Mean fiber area increases at first, but then deceases after the 16 day mark, suggesting larger fibers splitting into smaller fibers.

Additional studies have found evidence of fiber splitting post stretch in avian models (Antonio & Gonyea, 1994; Sola, Christensen, & Martin, 1973). Not all avian stretch studies showed evidence of fiber splitting however. Chicken ALD subject to stress stimuli gave 120% increase in muscle mass with a 130% increase in fiber area, the control, group which was not subject to stretch, showed the largest increase in fiber area however (Gollnick et al., 1981). The control group experiencing a higher rate of fiber splitting proves a great example of just how poor a state of understating we have about hyperplasia as a whole. Although there is evidence of stretch induced fiber splitting in quail and chicken, avian models are quite different from mammalian in regards to their overall muscle physiology.

1.1.2 Marine Models of muscle growth

Black sea bass exhibit muscle fiber splitting in order to relieve the constraints of metabolic diffusion (Figure 2). The muscles of the black sea bass grow hypertrophically until they reach a diffusion limitation of aerobic metabolism, at which point the onset of hyperplasic growth is observed. Although there are nuclei throughout the center of the cell, the vast majority are localized to the periphery (Priester, Morton, Kinsey, Watanabe, & Dillaman, 2011). Much like in mammals, the black

sea bass reach a limit in which their myonuclear domain is too large to accommodate the basic needs of the cell. Such a behavior is very similar to that suggested by Antonia and Gonyea with their work on quail ALD.

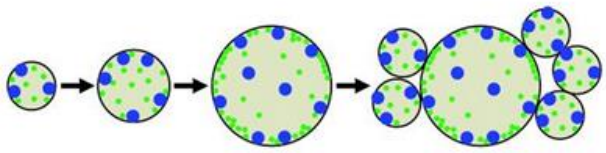

Figure 2. Hyperplasic muscle growth in Black sea bass, Kinsey et al (2010)

The blue crab dark muscle fibers exhibit an interesting form of muscle fiber segmentation in which the fibers develop intracellular perfusions (Figure 3). Each individual subunit represents one metabolic functional unit, similar to the idea of a myonuclear domain. Although the fiber is segmented into smaller sub-units, the fiber as a whole remains as the contractile unit (Priester et al., 2011). Such a division is not necessarily fiber splitting, but it is definitely germane to the topic of myonuclear domain and its relation to skeletal muscle hyperplasia.

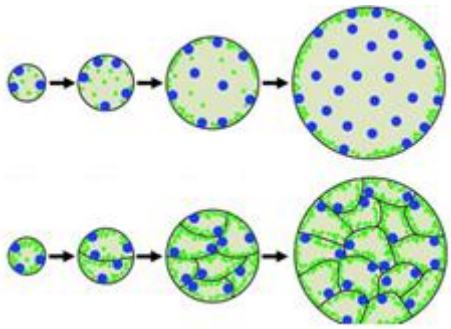

Figure 3. Development of intracellular perfusions in crab muscle, Kinsey et al (2010)

In both the black sea bass, and the blue crab models, we see a shifting of organelles in relation to fiber size. As fiber size increases, Mitochondria move from a uniform distribution to clustering primarily at the sarcolemma (Jones, Gittins, & Hardy, 2009). The mitochondria are most likely moving closer to the sarcolemma to get closer to their substrate, O_2. The move to the sarcolemma causes a subsequent increase in diffusion distance of ATP, suggesting the diffusion of O_2 is a much larger constraint to their overall cellular function.

1.1.3. Experimental models of muscle growth in mammals

A major component of studying mammalian skeletal muscle growth via hyperplasia is the level of exercise intensity. High intensity training causes muscle fiber hyperplasia at rates higher than that seen in lower intensity training (Gonyea et al., 1986). Humans often undergo high intensity training and one would be tempted to label them a great experimental model. Removal of as much tissue as possible after overload will greatly enhance the quality of the experiment. More tissue to work with will give more fibers to analyze, thus increasing your chances of finding morphological anomalies. It would be unethical to permanently impair the functionality of a human, and for this reason they do not make ideal models.

Many models have been trained to perform exercise, but no model is perfect. One common method of training is pain aversion, a model in which an animal is given a painful stimulus and must move away from said stimulus while affixed to a weight, thus exerting extra force on the animal and in essence, training it (Figure 4). This method, like most pain aversion methods, requires very specialized equipment and many would argue is rather barbaric and unethical.

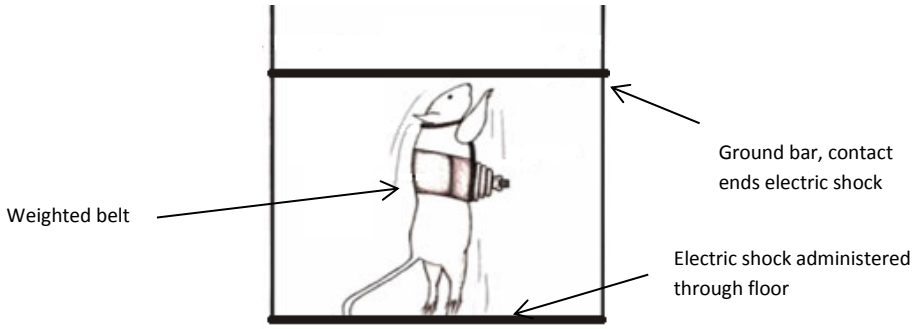

Figure 4. Exercise induced via aversion to painful stimuli (Ho et al., 1980). A weighted belt is attached to a rat, an electric current in applied through the floor and the rat must stand to touch a bar in order to stop the painful stimuli.

Classical conditioning by means of food reward is an often used method to stimulate muscle growth via hyperplasia. An animal is given a food reward in response to performing a task requiring exercise (Figure 5). In this model, the animal does not incur any direct and intentional physical pain, but it is still subject to psychological stress. There is still a need for very specialized equipment and training.

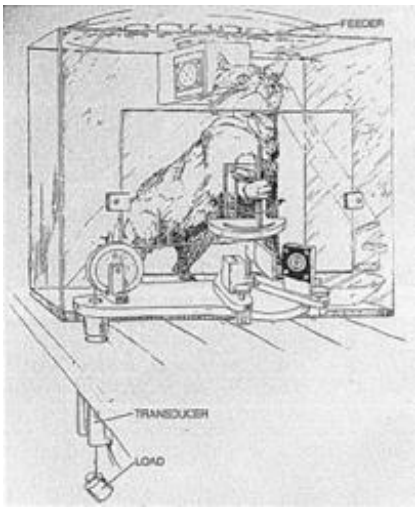

Figure 5. Exercise induced via food reward (Gonyea, 1980). A cat is conditioned to move a bar with its forearm. Weights attached to the bar via pulley act as resistance and require exercise by the cat, thus overloading the FCR.

Surgical ablation is a very common method of simulated exercise. Muscles will often work in pairs to alleviate the workload on one muscle, these pairs are termed synergists. A muscle can be overloaded if its synergist is surgically removed, resulting in an increased load on the remaining muscle. Synergist ablation would seem to be the most practical in terms of reproducibility, and time required per test animal. For these reasons, we elected to use surgical ablation to stimulate overload and potentially muscle hyperplasia.

1.2 Aims of study

- Investigate the roll of skeletal muscle fiber hyperplasia in relation to muscle growth
- Study the incidence of split fibers following muscle overload
- Study the physiological mechanisms behind fiber growth

2. Materials and Methods

2.1 Experiments on animals and tissues

2.1.1 Animals

The experiments were performed at the Department of Biosciences (IBV) at the University of Oslo, Norway, under direct approval of The Norwegian Animal Research Committee (FDU). Pax7-DTA mice were used. Treatment, housing, and feeding of all experimental animals were in accordance with the criteria set out by the EU and FDU. The mice were housed on a reversed 12 hour light/dark cycle. The temperature in the housing container was maintained at 21±1°C, with a ventilation rate of 5-20 times per hour, and a humidity level of 55±10%.

2.1.2 Surgical procedures

All animals were anaesthetized with Isoflourane (Baxter, Oslo, Norway) mixed with standard air at a flow rate of 5-6 L/min. The mice were placed in an induction chamber filled with 5% isoflourane in order to induce anesthesia. A pinch sufficient to elicit a retraction reflex was delivered to the metatarsus region to ensure sufficient anesthesia. Following successful anesthesia, the mice were transferred to an operating pad. Anesthesia was maintained with the aid of a mask delivering isoflourane at a concentration of 2-2.5%. Respiration frequency was monitored, alongside intermittent metatarsus pinching to ensure sustained anesthesia.

2.1.3 Synergist Ablations

Anaesthetized mice were prepped for surgery by shaving the left hind limb with a commercially available animal hair trimmer. Following shaving, a hair removal cream (Boots) was applied to the left hind limb and allowed one minute to sit before removal of cream and subsequent hair. The left hind limb was then washed with 70% ethanol and fixed to the surgical mat. An incision lateral to the tibia was made to surgically expose the TA muscle. The TA tendon was identified and severed. Approximately 80% of the TA was removed to induce overload of the synergist muscle, the EDL (Figure 6). Drying of the muscle was prevented by periodically applying ringer acetate solution (131323, B. Broun Petzold).

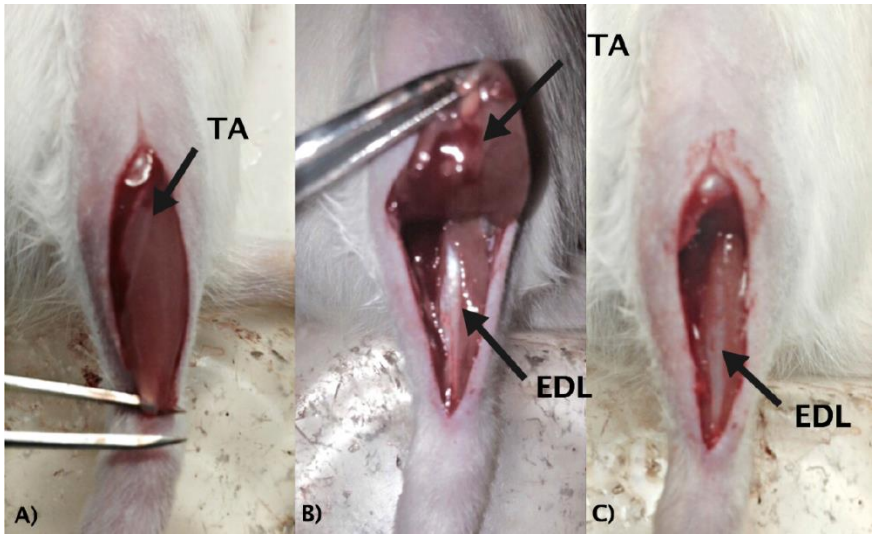

Figure 6. Synergist ablation, (Alver, 2014) A) Identification of the distal TA tendon. **B)** The distal tendon is then cut and roughly 80% of the TA is excised to induce overload of the EDL muscle. **C)** The EDL muscle is clearly visible following removal of the TA.(Alver, 2014)

2.1.4 In vivo transfection/Electroporation

In order to better visualize the structure of the individual myonuclei, a skeletal muscle specific alpha actin promoter was used to drive the expression of fluorescent mCherry with a nuclear localization signal (mCherry-NLS). The expression cassette was inserted into a pECFP-Nuc (Clontech loboratories inc) backbone. In order to visualize the plasma membrane, an expression vector (pCDNA3, Invitrogen) containing a CMV promoter, was used to drive the expression of Myrpalm. Both plasmids were previously constructed by the Gundersen group.

Gene transfer into muscle is very inefficient; electroporation has been shown to greatly increase this rate of transfection (Aihara & Miyazaki, 1998). Electroporation is a technique in which an electric current is passed through cells to facilitate the uptake of plasmid DNA. The process is thought to induce permeabilization by creating small poles in the plasma membrane, and by electrophoresis which moves the DNA into the cell (Lu, Bou-Gharios, & Partridge, 2003; Somiari et al., 2000). Following removal of the TA, *in vivo* transfection/electropermeabilization of plasmid DNA was performed as described by Mathiesen (1999). An insulin syringe (0.3ml, BD Micro-Fine™, VWR) was used to inject 20µl of a 0.5µg/µl DNA solution into center of the EDL. Following DNA injection, two silver electrodes (1cm long and 1mm thick) placed 1-2 mm apart, were placed at 4 different locations along the EDL. At each location, an electric field was applied using a pulse generator (Pulsar 6bp, Fredrick Haer & Co). 1 train with 1 second intermission was applied at each of the 4 locations on the muscle, each consisting of 1000 bipolar pulses with amplitude of 150V/cm, 200µs in each direction. The electrical charge was registered by an analogue oscilloscope (03245A, Gould Advance). Mice were then sutured and allowed to recover in their cages.

2.1.5 Maceration

Muscles bound for fiber teasing were removed and placed in a paraformaldehyde bath. Muscles were lightly stretched to approximate *in situ* length, and allowed to stand for 48 hours. Muscles were then transferred to 2ml microtubes (PP, Sarstedt) and suspended in 40% NaOH for 3 hours. Muscles were then transferred to new microtubes containing 20% NaOH for 7 minutes. Muscles were then washed with ultra-purified Milli-Q water 3 times and stored at 4 °C.

2.1.6 Fiber teasing

Following maceration, the EDL was roughly broken into individual fibers. The macerated muscle sample was poured into a glass petri dish to allow fiber separation. Fibers were then taken from the dish and placed onto superfrost glass slides (Thermo Fisher Scientific, Oslo, Norway). Fibers were separated from one another manually with high precision tweezers. Once a desired number of fibers have been isolated (roughly 20-40) the slide was allowed to dry at room temperature overnight.

2.1.7 Perfusion

To maintain muscle integrity throughout maceration the muscles were fixed *in vivo* via whole body perfusion. This technique was only implemented for the samples bound for maceration, those bound for sectioning were flash frozen in a buffer of 2-methylbutane cooled with liquid nitrogen. A lateral incision through the integument and abdominal wall was made just beneath the rib cage (Figure 7A.). The Diaphragm was severed to expose the pleural cavity. The rib cage was removed by two cuts from the primary lateral incision to the collar bone, one cut for each side of the abdomen (Figure 7B). The sternum was then lifted and removed to expose the heart (Fig 7C). A needle was inserted into the posterior end of the left ventricle. A 20ml syringe was attached to said needle. An outlet was produced in the right atrium to allow an exit through which the blood and fix may flow (Fig 7D). Pressure was applied to the syringe and fix was gradually pushed throughout the mouse circulatory system, fixing the tissues of the animal.

A). **B).** **C).**

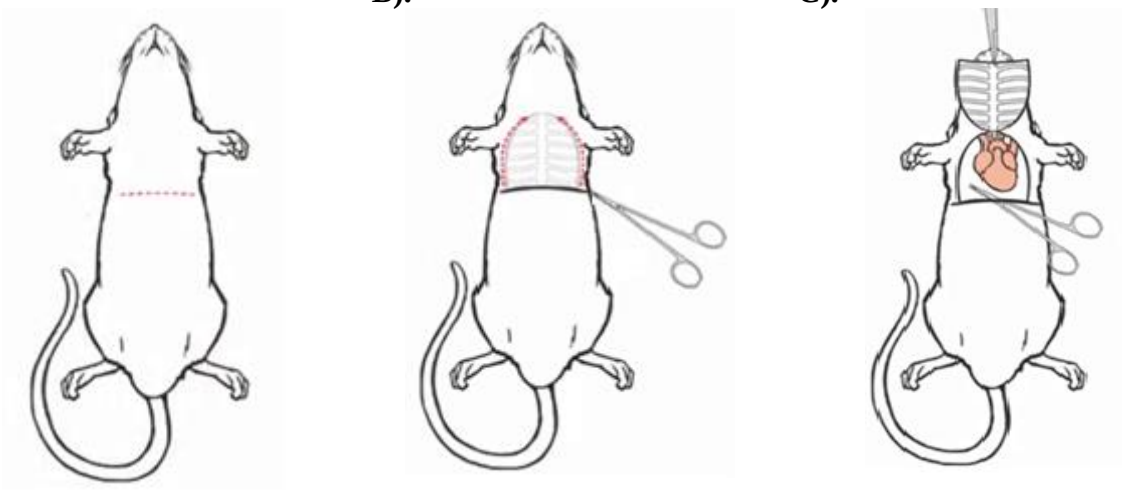

D).

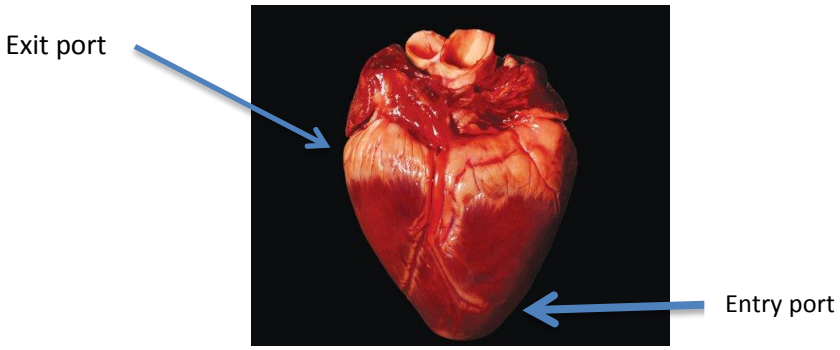

Figure 7. Circulatory perfusion. A). Opening of the pleural cavity. **B).** Separation of the rib cage. **C).** Removal of the rib cage to expose the heart. **D).** Entry and exit ports installed into the heart, photo provided by Popular Science Magazine.

2.1.8 Measurements of cross sectional area

Human bias was prevented by randomly assigning file names to the images. All digital analysis on images was done in Photoshop CS6 (Adobe Systems, San Jose, CA, USA). Random selection of muscle fibers was achieved by using a grid to select muscle fibers, thus eliminating any possibility of human bias (fig 8). Muscle fiber cross sectional area (CSA) was measured by tracing the cell membrane and allowing Photoshop algorithms to calculate a value. A pixel value was calculated by use of a scale bar to convert square meters into pixels.

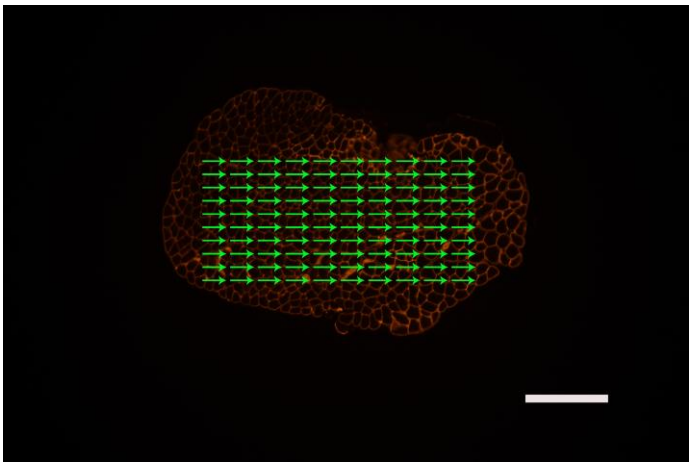

Figure 8. Muscle section isolated from EDL stained with laminin (red), image taken using 4X objective. Grid (green) shows method for unbiased fiber selection. Scale bar = 100μm

2.1.9 Analysis of collagen and dystrophin dissimilarities

The Gundersen group has observed a different time line of regeneration for collagen and dystrophin following exercise-induced necrosis during previous experiments. These reports are unpublished, and little research has gone into this phenomenon. The rationale behind this was that if small clusters of fibers recognized by dystrophin staining were all inside a common collagen ring, this would indicate that these fibers in fact were regenerating from one fiber. It was decided to follow up on these observations by staining for both collagen and dystrophin in overloaded tissue and analyzing the results. Samples were imaged and imported into Photoshop for analysis and identification of any differences in staining. Each different stain had its color profile isolated and inserted into the color channel of a new image allowing for the images to be overlapped (Figure 9).

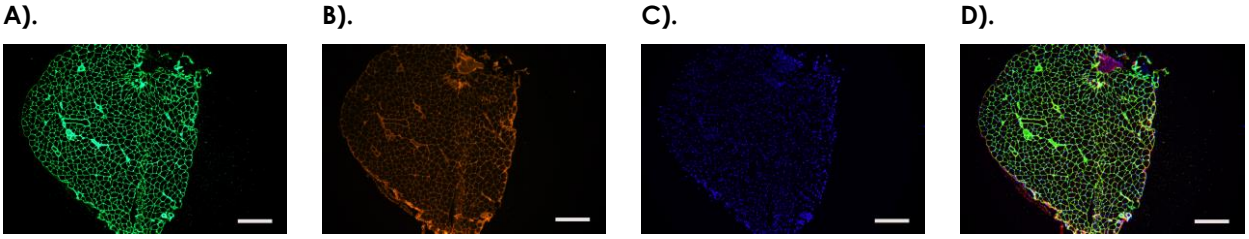

Figure 9. Cryo-sectioned EDL stained with antibodies against collagen **(A)**, dystrophin **(B)**, and hoechst **(C)**. The images were then merged **(D)** in Photoshop to more easily view differences in staining. All images taken using 4X objective. Scale bar = 100μm

2.2 Histology

2.2.1 Removal of muscles

The EDL was removed at 14, 21, 28, and 35 days after overload, depending on the time group to which the animal belonged. The animals were placed under anesthesia, with Isoflourane. Once the mouse was unconscious 0.1ml ZRF cocktail was injected into the abdomen to ensure deep and sustained anesthesia. The EDL of both the experimental left hind leg, and the control right hind leg were removed for downstream analysis.

2.2.2 Snap-freezing of muscles

Muscles bound for cryo-sectioning were placed inside a rubber boat and suspended in O.C.T. compound tissue-tek (Sakura). Muscles were stretched slightly, to approximate *in situ* length and secured with pins. The samples were then placed in a beaker containing 2-Methylbutane (Sigma-Aldrich) cooled to -160°C, by means of a liquid nitrogen bath. After 15-20 seconds immersion in cooled 2-Methylbutane, samples were transferred to 2ml microtubes (PP, Sarstedt) and stored at -80°C until sectioning.

2.2.3 Cryo-sectioning

The frozen muscle samples were sectioned into 10 µm thick cross sections using a cryostat (CM1950, Leica Biosystems). Samples were maintained at -21°C throughout sectioning. Sections were placed on superfrost glass slides (Thermo Fisher Scientific, Oslo, Norway) and allowed to dry at room temperature. To ensure sample protection slides were surrounded by lens paper and wrapped in aluminum foil prior to storage at -80°C.

2.2.4 Staining with haemotoxylin

Haemotoxylin is a naturally occurring compound found in the logwood tree. It is a basic compound which binds to acidic compounds containing negative charges to form salts. Haemotoxylin allows for visualization of muscle striations, allowing one to further study bifurcated fibers. Roughly 1mL of Gills Haemotoxylin (Sigma) was applied to each slide of teased fibers and allowed to sit for 20 minutes before 3 subsequent washes with PBS. Samples were then viewed under a light microscope to study possible split fibers.

2.2.5 Staining with hoechst

Hoechst (33258 Sigma) is a fluorescent dye that binds the minor groove of double stranded DNA, allowing for its visualization. Hoechst is excited by ultraviolet light at around 350nm and emits a blue fluorescent light at around 461nm. Both teased fiber samples, as well as cross sectioned fiber samples were stained with Hoechst for nuclear imaging. Enough hoechst-solution to completely submerge the samples was applied for roughly 5 minutes prior to imaging.

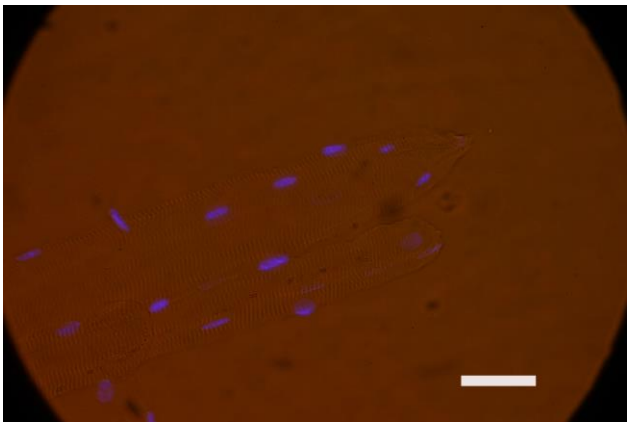

Figure 10. EDL micrograph of a muscle fiber stained with hoecsht (blue), Imaged through a 40X objective, scale bar = 10µm

2.2.6 Staining for laminin

Laminin is a protein found in the extracellular matrix and is a major component of the basal lamina in muscle fibers. Muscle sections were first stained with a polyclonal antibody targeted to laminin (L9393, Sigma). The sample was then stained with a secondary antibody conjugated to the flourochome TRITC (T6778, Sigma) to visualize the primary antibody binding to the basement membrane of the muscle fibers (Figure 11).

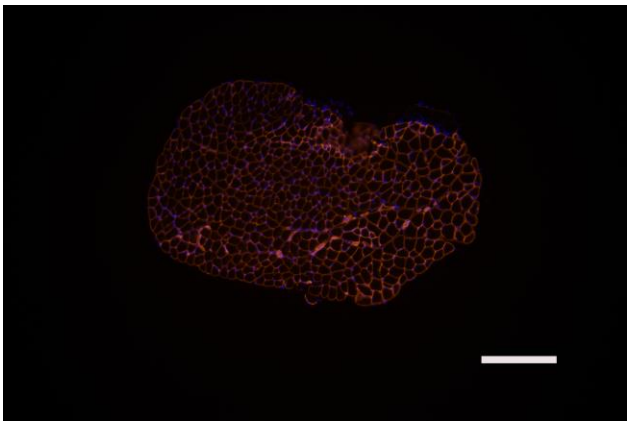

Figure 11. Micrograph of cryo-sectioned EDL stained with antibody against laminin (red) and hoechst (blue). Imaged through a 4X objective, scale bar = 100µm

2.2.7 Staining for phalloidin

Phalloidin is a phallotoxin, found naturally in the death cap mushroom (amanita phalloides). Phalloidin is known to bind and stabilize F-actin (filamentous actin) and prevents the depolymerization of actin fibers. The affinity of phalloidin for actin makes it both poisonous and rather useful as a stain against actin. To better visualize fiber bifurcation, whole fiber samples were stained with phalloidin (A12381, Life technologies). The phalloidin used was an F-actin probe conjugated to Alexa flour 594 (red). Samples were treated with permeabilization buffer prior to staining with phalloidin. Muscle samples were then washed with PBS prior to imaging.

2.2.8 Staining for Collagen and dystrophin

Collagen is the main component of connective tissue, and thus the most abundant protein found in mammals. Dystrophin is a cytoplasmic protein, which is a vital component of the costamere. The two express in roughly the same area surrounding the cell. It has been shown that cells can survive in the absence of some forms of collagen, suggesting that dystrophin plays a more integral role in fiber stability, and may thus develop before collagen (Grumati et al., 2010). We hoped that staining for collagen and dystrophin concurrently could give us the opportunity to see if there are muscle fibers expressing dystrophin but not collagen, such a disparity could suggest the formation of a new fiber. Cross sectioned samples were stained against both collagen (ab19808, Abcam) and dystrophin (D8168, Sigma). Samples were allowed to incubate overnight and then washed before staining with fluorophores Alexa 488 (green) for collagen and TritC red (Life technologies) for dystrophin. Following an additional overnight incubation of secondary antibodies, the samples were imaged.

2.3.9 Fluorescent microscopy

The samples stained using fluorophores were imaged at 4X, 10X, 20X, 40X and 60X magnifications using a camera (Canon 60D) attached to microscope (BX50W1 Olympus). The 20X, 40X, and 60X magnified images were taken through a water immersion lens.

2.3.10 Confocal microscopy

An anaesthetized mouse was placed on a surgical plate, and the EDL was exposed and covered with a glass slide. The mouse was then viewed using a confocal microscope (Olympus BX61WI, Tokyo, Japan) connected to an imaging system (Olympus fluoview FV1000, Olympus, Europe GmBH).

2.4 Statistical procedures

All statistical procedures were performed using the program Prism (Graphpad, La Jolla, CA, USA). To determine statistical significance of EDL cross sectional area, a Kruskal-Wallis one-way analysis was performed with a Dunn's multiple comparisons post-test. Statistical significance of macerated fiber count was determined using a T-test.

3 Results

3.1 Measurement of cross sectional area

CSA measurements of the EDL revealed that the trained group had a 56% increase in size when compared to the control group after 2 weeks (P< 0.0001). 3 weeks after ablation there was a 55% increase (P< 0.0001). Week 3 was the only week not to show a higher increase than the previous week. There was a 57% increase after 4 weeks (P< 0.0001). 5 weeks post ablation there was a 59% increase in fiber CSA for (P< 0.0001) (Figure 12).

A).

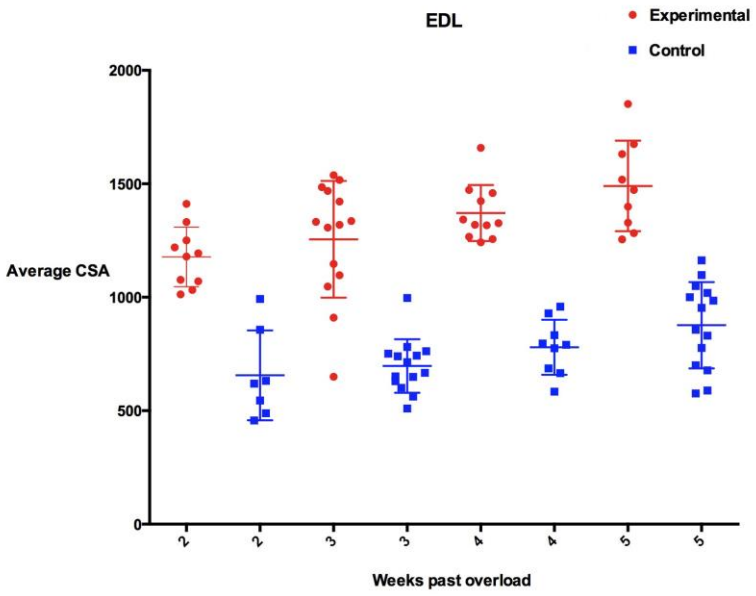

B).

Week	Mean CSA (Experimental)	SEM (Experimental)	Mean CSA (Control)	SEM (Control)	Total Increase
2	1178	41.61	656	74.86	56%
3	1255	68.69	697	31.54	55%
4	1371	37.23	780	40.41	57%
5	1491	66.46	876	50.83	59%

Figure 12. Figure shows cross sectional area measurements (CSA) of the EDL. **A)** Each dot represents one EDL muscle in each group (n=8-12). Each muscle CSA mean is calculated from n=100 fiber measurements. **B)** Table of data shown in **(A)** with total increase in experimental compared to control shown, and SEM.

To further investigate muscle fiber size increases, CSA measurements were compared in an animal to animal manner (Figure 13). The average difference in size between control and experimental muscle from individual animals was taken. The individual averages were then themselves averaged to give an average size difference for each time group. After 2 weeks there is a 47% increase in fiber size from control to experimental, this number drops each successive week to settle at a 39% increase for week 5.

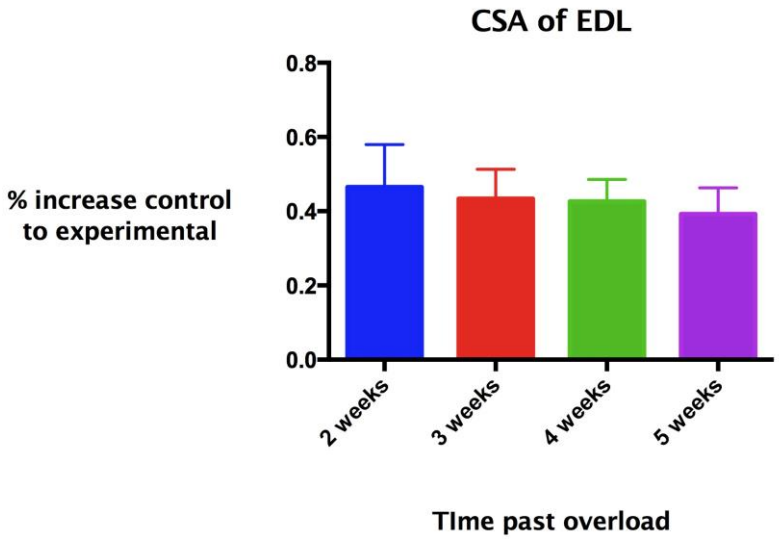

Figure 13. Animal to animal comparison of CSA in the EDL muscle. Week 2 showed a 47% increase in size. Week 3 showed a 43% increase in size, Week 4 showed a 42% increase in size. Week 5 showed a 39% increase in size. Ordinary one way ANOVA test determined that the difference in mean among data groups was not statistically significant. P value = 0.3591.

3.2 Frequency distribution of fiber cross sectional area

It was believed that an increase in split fibers could be accompanied by an increase in the number of smaller fibers as compared to large fibers. To assess this possibility, a frequency distribution was made for each time group (Figure 14). Within each time group 100 fibers were measured from 7-14 mice, depending on the group.

A.) 2 weeks post overload

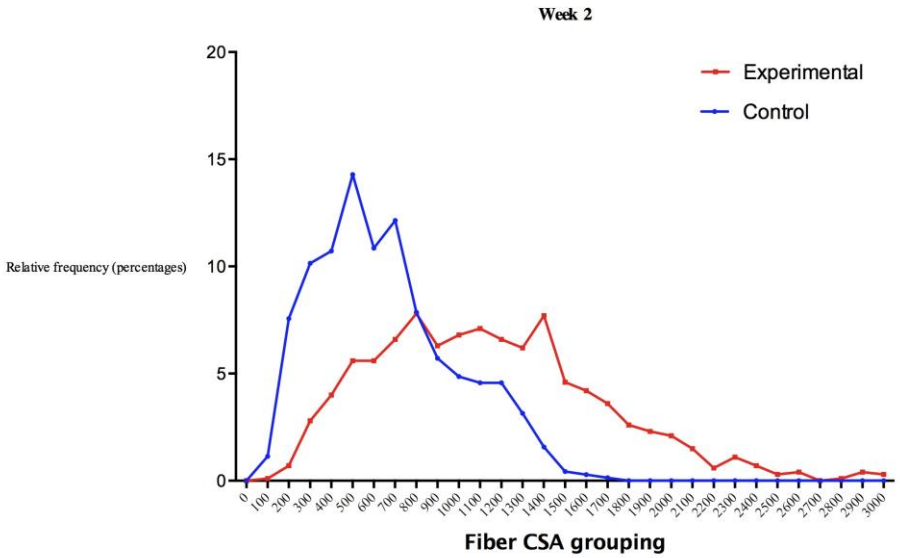

B.) 5 weeks post overload

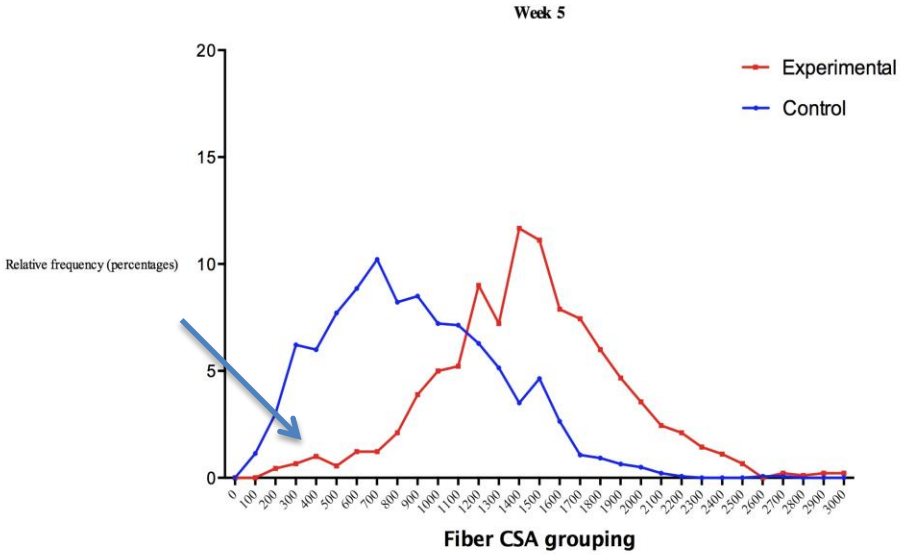

Figure 14. Figure shows cross sectional area measurements (CSA) of the EDL mapped out according to their frequency. Y-axis represents a percentage out of 100, while the X-axis represents size groups in μm². Each dot represents the percentage of fibers which fall into the given CSA size groups on the X-axis. Each muscle CSA mean is calculated from n=100 fiber measurements. **A).** n = 7 mice. **B).** n = 9 mice. The arrow in **(B)** indicates a population of small fibers which may account for some perceived fiber splitting.

3.3 Maceration and Fiber teasing

Visual analysis of individual muscle fibers revealed several incidences of bifurcation. The results showed an increase in split fibers in the experimental groups compared to the control (Figure 15). After two weeks 1.83% of all fibers were split for the experimental group, and 1.4% of all fibers were split for the control group. By week 5, 3.6% of the fibers were split for the experimental group, and only 1.47% of fibers were split for the Control group.

A)

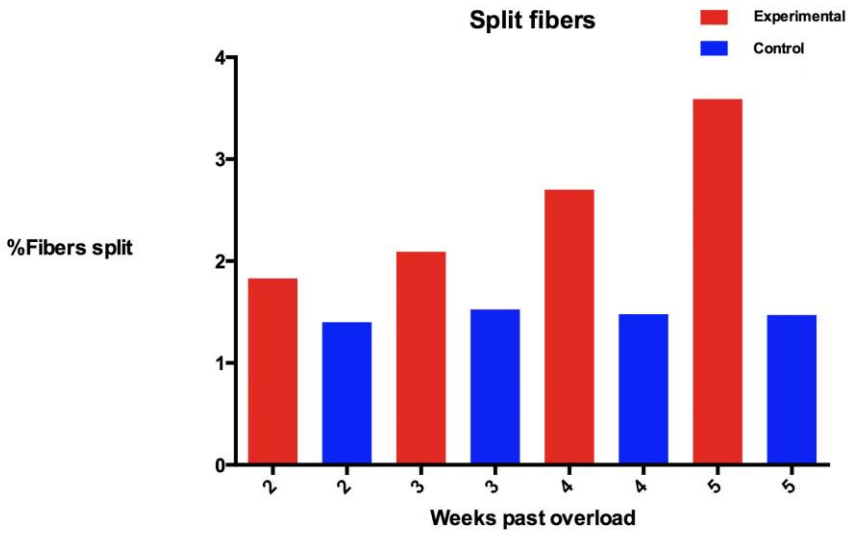

B)

Group	Number of split fibers	Number of non-split fibers	Percentage of Split fibers
2 weeks Experimental	11	600	1.8%
2 weeks Control	8	571	1.4%
3 weeks Experimental	13	621	2.1%
3 weeks Control	9	590	1.5%
4 weeks Experimental	16	609	2.6%
4 weeks Control	8	540	1.4%
5 weeks Experimental	22	612	3.6%
5 weeks Control	9	613	1.5%

C).

1.

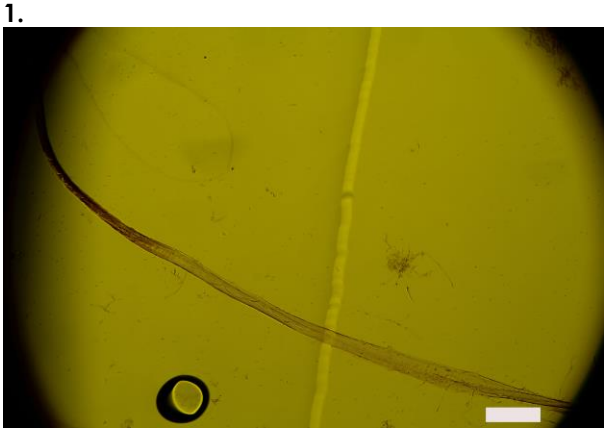

2.

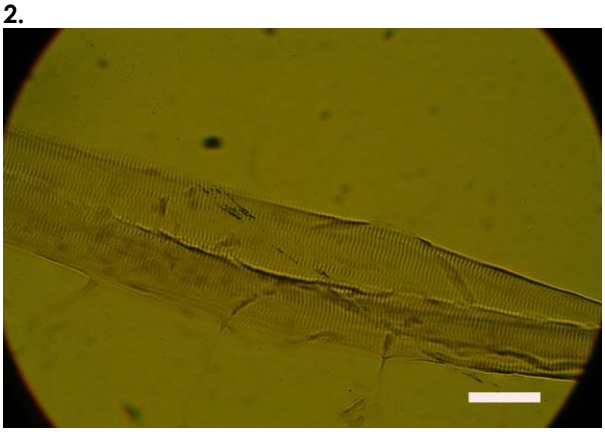

3.

4.

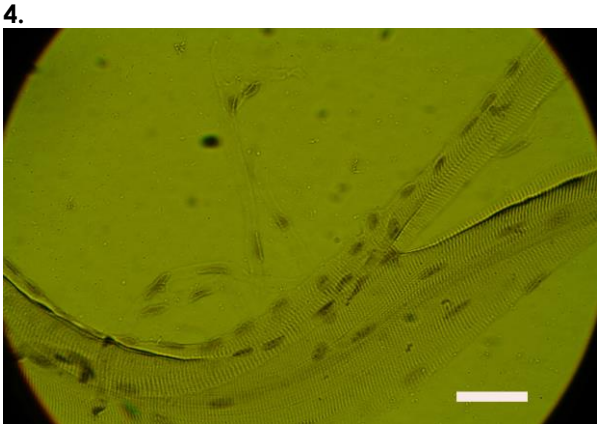

5.

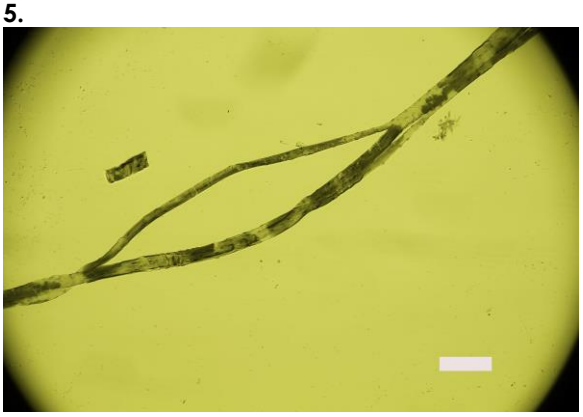

6.

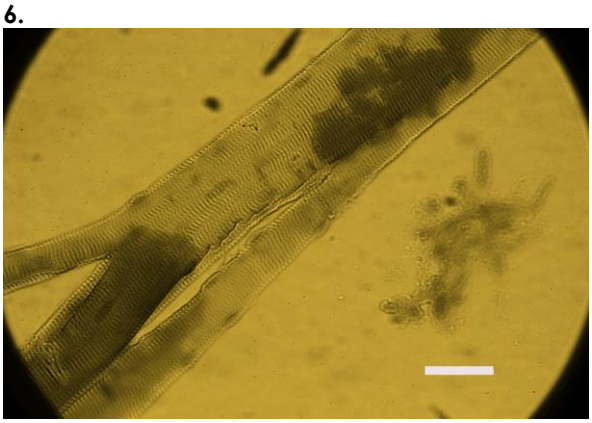

Figure15: Incidence of Fiber splitting in trained vs untrained EDL. A) Fibers were assessed for possible splitting and sorted into either split, non-split categories. Y-axis represents the percentage of split fibers to normal fibers. Percentages are calculated using (n=540-613), depending on group, P value = 0.0326 **B)** Raw data on total fiber number compared to split fiber incidence. **C)** Images showing bifurcated fibers suspected of being split. 1,3, and 5 were imaged through a 10X objective lens, scale bar 0 30 µm. 2,4,and 6 were imaged through a 40X objective lens, scale bar = 10µm.

3.4 Electroporation and plasmid transformation

Due to the low incidence of split fibers as well as the low incidence of successful plasmid transfection and expression, no quantifiable results were achieved by this method. Although nothing relating to fiber splitting could be obtained from the images, the transfections were successful.

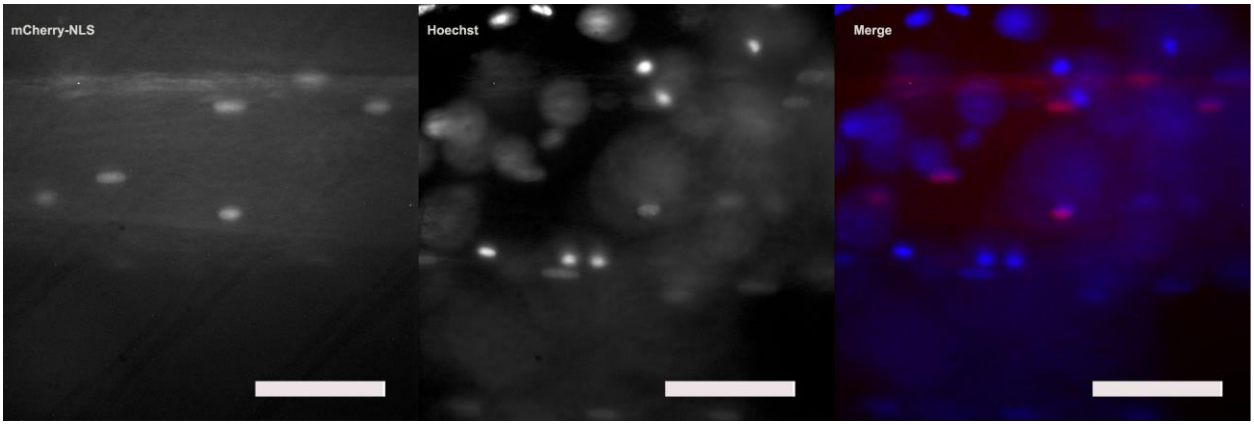

Figure 16. Muscle fiber expressing mCherry (red), and hoechst (blue). Imaged through confocal microcopy with a 20X objective, scale bar = 10μm

3.5 Collagen and dystrophin staining

Staining EDL samples for collagen and dystrophin failed to give any noticeable differences. Cryo-sectioned samples of plantaris, overloaded by synergist ablation of gastrocnemius and soleus were obtained from concurrent experiments in the Gundersen lab. The lab has noticed a larger hypertrophy in the plantaris, compared to the EDL. For this reason we selected to try differential collagen and dystrophin staining on plantaris. Fiber sections were stained with collagen and dystrophin to examine possible discrepancies in their staining. 2 groups were used, 2 and 3 weeks post overload. Week 2 showed 2 staining inconsistencies, while week 3 showed 6. Every staining inconsistency was found in an experimental section, no differences were found in the control group.

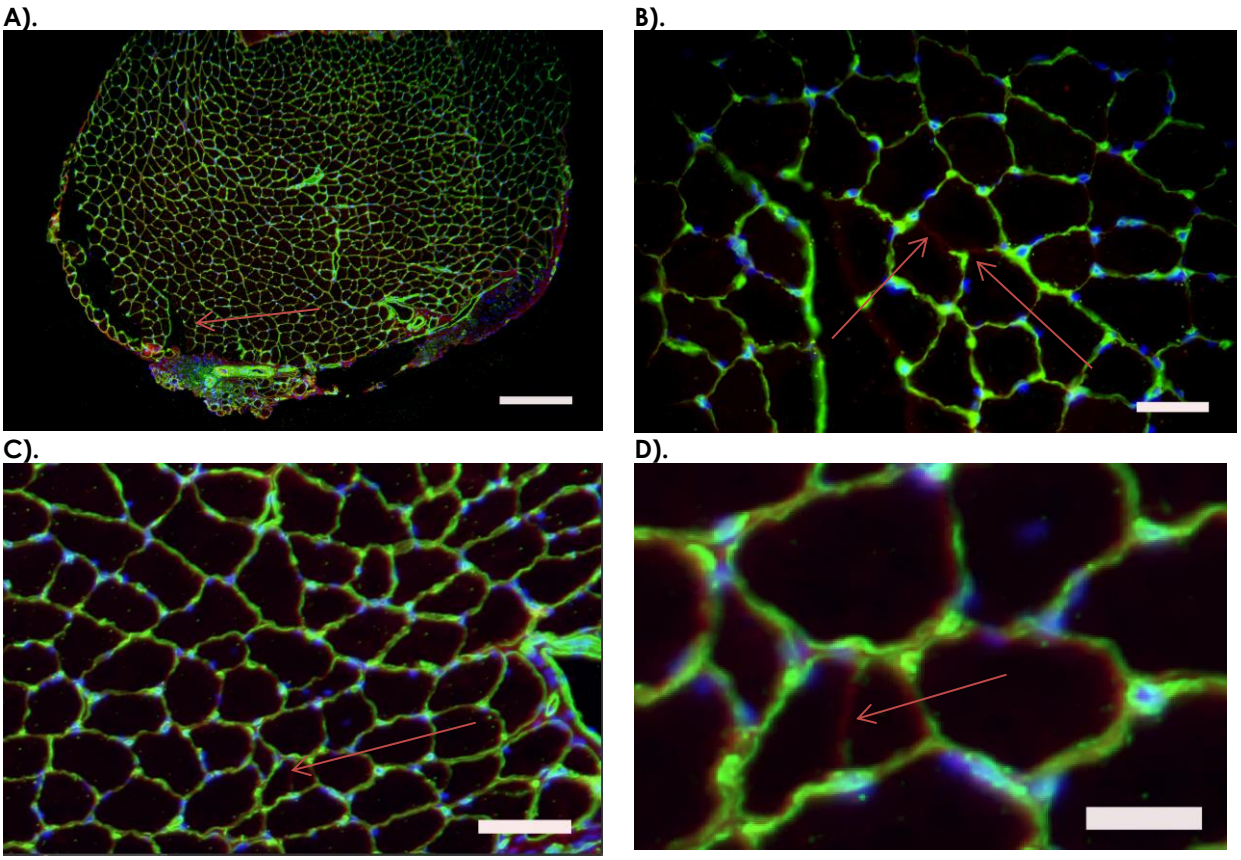

Figure 17. Micrograph of plantaris, cryo-sectioned and stained with antibody against collagen (green), dystrophin (red), and hoechst (blue). Differences in staining between collagen and dystrophin are visible by arrow. **A).** 10X magnification, scale bar = 100µm. **B).** 40X magnification, scale bar = 10µm. **C).** 40X magnification, scale bar = 10µm **D).** 60X magnification, scale bar = 5µm.

4 Discussion

4.1 Muscle overload results in a very low level of fibers with a split appearance

Five weeks after overload, we saw a split appearance in 3.6% of the fibers (Figure 15B). Previous reports using the murine model have found rates of splitting as high as 9.6% (Ho et al., 1980). Our level of hypertrophy however was quite high at 39% at the end of the experiment. Previous studies have shown notably lower gains in CSA (Gollnick et al., 1981). There have been many reported cases of Hypertrophy and indeed Hyperplasia at a much higher rate than that seen in our report, but they have mostly come from induced stretch avian models (Antonio & Gonyea, 1993, 1994; Hall-Craggs, 1972; Holly, Barnett, Ashmore, Taylor, & Mole, 1980; Sola et al., 1973). Due to the inherent differences in muscle physiology and metabolism, the avian model and mammalian model should not be directly compared (Maier, 1997). Previous experiments on training in humans have produced an increase in fiber area lower than our reported 39% after 31 days, 17% (Kadi et al., 2004), 9.9% (McCall et al., 1996) and 22.8%(Cureton, Collins, Hill, & McElhannon Jr, 1988).

Concurrent with the low incidence of split fibers, our fiber frequency distribution is not consistent with that of a large increase in newly formed fibers (Figure 14). As a fiber splits it necessarily must decrease in size, as well a new fiber necessarily must be smaller than a mature fiber as it has not had time to grow. If there were significant fiber splitting or novel fiber development taking place, one would expect an increase in the frequency of very small fibers. This however, does not seem to be occurring within our results. From week 2 to week 5 the graph has shifted to the right in the experimental group indicating an overall increase in average fiber size. The control group has a less dramatic shift from week 2 to week 5, but there is still a general shift to the right, indicating a larger amount of fibers of larger CSA. The population of very small fibers present in Figure 14B could correlate to the perceived split fibers observed. The small peak relates to 1.5% of the total fibers. Manual fiber teasing found 3.6% of fibers to be split in the experimental group after 5 weeks (Figure 15B). The small peak seen does represent a population of small fibers and could correlate to the incidence of split fibers seen in Figure 14B.

4.2 Explanation to the observed fiber bifurcation

Although it was shown that overload resulted in an increased incidence of muscle fibers with a split appearance, it cannot be said with certainty that this was the result of muscle fiber splitting. The mere appearance of bifurcation could be explained as fiber splitting, novel fiber formation, or even simple mechanical tearing from human handling. Great care was taken when handling the fibers, so human intervention and subsequent tearing is unlikely. Novel fiber formation however, is not as easily disregarded.

Ample evidence exists that animals are capable of regenerating large amounts of tissue following injury. Salamanders for example, have the ability to regrow entire limbs after losing them to trauma. The salamanders regeneration process seems to be mediated by satellite cell activation (Morrison, Lööf, He, & Simon, 2006). Mammals cannot regrow such complex structures as entire limbs following injury, but they have been shown to regrow muscle tissue. Small mammals (rats) have been shown capable of entire muscle regeneration after surgical intervention. A muscle is removed, chopped into many smaller pieces and placed back in the animal, ultimately resulting in whole muscle regeneration. This process has been shown to be caused by satellite cell activation (Carlson, Hsu, & Conboy, 2008).

As previously stated, the satellite cell is a muscle precursor cell which can give rise to new myonuclei to aid in decreasing the myonuclear domain. The satellite cell has also been shown to be the principle cellular source of myoblasts, which ultimately give rise to new muscle fibers (Figure 18)(Zammit, 2008; Zammit, Partridge, & Yablonka-Reuveni, 2006). Perhaps fiber splitting was in fact not the cause of our perceived bifurcated fibers, but instead it was damage induced muscle fiber regeneration mediated by satellite cell proliferation.

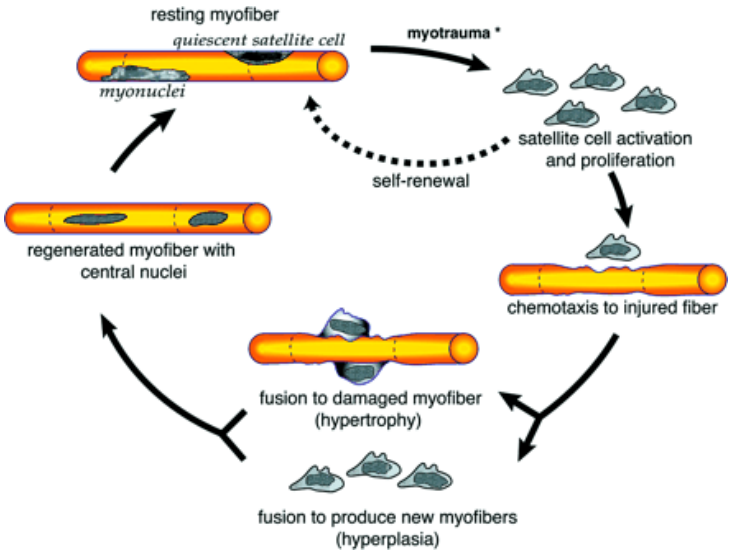

Figure 18. The role of satellite cells in muscle regeneration(Hawke & Garry, 2001).

4.3 Possible regeneration

Cryo-sections labeled with collagen and dystrophin resulted in some differential staining. As time past overload increased, the incidence of differential staining increased. Due to the low incidence of differential staining it is extremely unlikely that the stain itself is at fault for the observed differences. With the information at hand, there is no way to know for certain just what caused the differential staining, but a likely explanation is either fiber splitting, or novel fiber formation. There are two ways to think about muscle fiber hyperplasia, as regeneration, which would produce a new fiber or possibly even fibers with a split appearance, or as a growth phenomenon in which a large fiber splits due to size constraints. Although we cannot know for sure, our results, along with the unpublished accounts of previous Gunderson group experiments could imply regeneration.

If one muscle fiber were to split into two new fibers, one would expect the dystrophin layer of the two new fibers to form before the collagen layer. This is due to the location of dystrophin in relation to collagen. Collagen is an ubiquitous extracellular matrix protein (Lampe & Bushby, 2005), and is thus highly expressed in the extracellular matrix. A crucial role of the Dystrophin Glycoprotein Complex (DGC) is to anchor the intracellular cytoskeleton to the extracellular matrix (Lapidos, Kakkar, & McNally, 2004). We see that DMD is encompassed by, and anchored into the extracellular matrix (Figure 19). Thus, it follows that a splitting fiber would form its DMD prior to the extracellular matrix, as if it were the other way around, the cell would have nothing with which to attach. Our collagen vs. dystrophin results would suggest possible fiber splitting, but the incidence is so low as to warrant some skepticism.

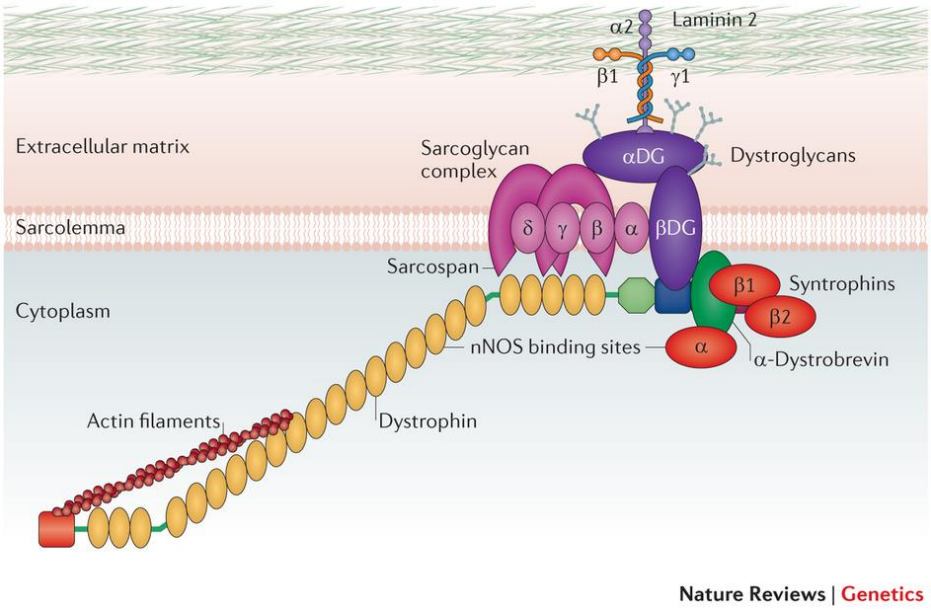

Figure 19. The location of collagen in relation to dystrophin(Fairclough, Wood, & Davies, 2013). From this picture we see that the DMD serves to connect the cytoplasm to the collagen rich extracellular matrix.

The surgery to remove the TA could have very possibly inadvertently damaged the EDL. Extreme care was taken to only remove the TA and to not jeopardize the integrity of any other tissues. However, the EDL necessarily underwent trauma when it was electroporated and thus could have triggered fiber necrosis and subsequent fiber regeneration. Perhaps the electric shock of the pulse generator used during electroporation could have been enough to critically damage the fibers in the EDL.

4.4 Unsuccessful Experiments

Staining with phalloidin proved unsuccessful and its results were thus removed from the thesis. Phalloidin stains F-actin and has been shown to stain whole fibers with high enough resolution to clearly see the striations (Hansen, 2009). Such a high resolution would allow one to differentiate between one muscle fiber that has split into two, and two muscle fibers which are simply very close together. We were unsuccessful in utilizing Hansen's method and used haemotoxylin instead. It is believed that our inability to stain with phalloidin was due to a problem of permeability. Our fibers were fixed *in vivo* via whole body perfusion and then allowed to sit in a fixative solution for 24 hours. Such a high level of fixation most likely proved impenetrable to the phalloidin stain, despite permeabilization of the fibers. The permeability problem was tested for by staining a cross sectioned sample (direct access to actin, no need for permeabilization of the membrane) and proved successful.

The plasmid chosen for transfection via electroporation proved successful. Fiber striations, as well as the contours and shape of the fibers expressing the plasmid DNA were clearly visible. The problem was the extremely low level of expression. Although electroporation has been shown to markedly increase the transfection efficiency of plasmid DNA into muscle tissue, a "good" transfection rate is around 10% (Mathiesen, 1999). In order to view the transfected muscle fibers, the muscle was exposed but kept within the mouse. This greatly reduces the amount of fibers visible to essentially just those present at the surface of the muscle. Upon imaging we were never able to make out more than 5 fibers per muscle. Seeing as our reported split fiber ratio was 3.6% at the highest, this makes the chances of finding a split fiber expressing our plasmid DNA extremely low.

4.5 Future directions and applications

To further investigate the roll muscle fiber hyperplasia plays in mammalian muscle growth, the experiment could be recreated with several tweaks to the method.

Electroporation gave no usable results and may very well have influenced our findings by inducing unwanted trauma. The expression rate of our transfected cells is so low, nothing short of significantly increasing the sample size would remedy the problem. Such a dramatic cost of animal life cannot be reasonably justified, thus transfection should be taken off the table. Additionally, replacing surgical overload for some form of food mediated training would cut down on trauma to the animal, and it has shown to produce both muscle fiber hypertrophy as well as hyperplasia(Gonyea, 1980; Gonyea et al., 1986). It may be helpful to supplement testosterone as well, as it has been shown to result in increased muscle hypertrophy (Bhasin, Woodhouse, & Storer, 2001; Hartgens & Kuipers, 2004; Sinha-Hikim, Roth, Lee, & Bhasin, 2003; Urban et al., 1995). Comparing these findings could give some insight into the role of fiber splitting/regeneration in relation to muscle growth.

MyoD, the master controller of myogenesis, plays a major role in regulating muscle differentiation (Singh et al., 2015). Staining cryo-sections with an antibody against MyoD could help support or refute the claim of novel fiber regeneration over fiber splitting. As a regenerating fiber will express MyoD at a detectable level (Anderson, McIntosh, Moor, & Yablonka–Reuveni, 1998). The Gundersen group is performing extensive research into the concept of myonuclear domain and muscle growth (Egner, Bruusgaard, Eftestøl, & Gundersen, 2013). Using their techniques to quantify the number of myonuclei in potentially split fibers and hypertrophic fibers and then comparing the two could reveal a possible relation between fiber hyperplasia, hypertrophy and myonuclear domain.

Ultimately a better understanding of muscle fiber growth, by means of hypertrophy, or hyperplasia, will increase our ability to treat muscular damage and disorders.

4.6 Conclusion

Muscle enlargement by overload is mainly caused by hypertrophy of existing fibers, but a role for hyperplasia under some conditions or in a longer timeframe not assessed in this thesis cannot be ruled out.

5 References

Adams, G. R. (1997). Role of insulin-like growth factor-I in the regulation of skeletal muscle adaptation to increased loading. *Exercise and sport sciences reviews, 26*, 31-60.

Aihara, H., & Miyazaki, J.-i. (1998). Gene transfer into muscle by electroporation in vivo. *Nature biotechnology, 16*(9), 867-870.

Alver, T. N. (2014). A physiological strength exercise model for rats.

Anderson, J. E., McIntosh, L. M., Moor, A. N., & Yablonka–Reuveni, Z. (1998). Levels of MyoD protein expression following injury of mdx and normal limb muscle are modified by thyroid hormone. *Journal of Histochemistry & Cytochemistry, 46*(1), *59-67*.

Antonio, J., & Gonyea, W. J. (1993). Progressive stretch overload of skeletal muscle results in hypertrophy before hyperplasia. *Journal of applied physiology, 75*(3), 1263-1271.

Antonio, J., & Gonyea, W. J. (1994). Muscle fiber splitting in stretch-enlarged avian muscle. *Medicine and Science in Sports and Exercise, 26*(8), 973-977.

Bhasin, S., Woodhouse, L., & Storer, T. (2001). Proof of the effect of testosterone on skeletal muscle. *Journal of endocrinology, 170*(1), 27-38.

Booth, F., Tseng, B., Flück, M., & Carson, J. (1998). Molecular and cellular adaptation of muscle in response to physical training. *Acta physiologica Scandinavica, 162*(3), 343-350.

Bruusgaard, J. C., Johansen, I., Egner, I., Rana, Z., & Gundersen, K. (2010). Myonuclei acquired by overload exercise precede hypertrophy and are not lost on detraining. *Proceedings of the National Academy of Sciences, 107*(34), 15111-15116.

Carlson, M. E., Hsu, M., & Conboy, I. M. (2008). Imbalance between pSmad3 and Notch induces CDK inhibitors in old muscle stem cells. *Nature, 454*(7203), 528-532.

Cureton, K. J., Collins, M. A., Hill, D. W., & McElhannon Jr, F. M. (1988). Muscle hypertrophy in men and women. *Medicine and Science in Sports and Exercise, 20*(4), 338-344.

Egerman, M. A., & Glass, D. J. (2014). Signaling pathways controlling skeletal muscle mass. *Critical reviews in biochemistry and molecular biology, 49*(1), 59-68.

Egner, I. M., Bruusgaard, J. C., Eftestøl, E., & Gundersen, K. (2013). A cellular memory mechanism aids overload hypertrophy in muscle long after an episodic exposure to anabolic steroids. *The Journal of physiology, 591*(24), 6221-6230.

Fairclough, R. J., Wood, M. J., & Davies, K. E. (2013). Therapy for Duchenne muscular dystrophy: renewed optimism from genetic approaches. *Nature Reviews Genetics, 14*(6), 373-378.

Gallanti, A., Prelle, A., Chianese, L., Barbieri, S., Jann, S., Schiaffino, S., . . . Moggio, M. (1992). Congenital myopathy with type 2A muscle fiber uniformity and smallness. *Neuropediatrics, 23*(1), 10-13.

Gollnick, P., Timson, B., Moore, R., & Riedy, M. (1981). Muscular enlargement and number of fibers in skeletal muscles of rats. *Journal of applied physiology, 50*(5), 936-943.

Gonyea, W. J. (1980). Role of exercise in inducing increases in skeletal muscle fiber number. *Journal of applied physiology, 48*(3), 421-426.

Gonyea, W. J., Sale, D. G., Gonyea, F. B., & Mikesky, A. (1986). Exercise induced increases in muscle fiber number. *European journal of applied physiology and occupational physiology, 55*(2), 137-141.

Grumati, P., Coletto, L., Sabatelli, P., Cescon, M., Angelin, A., Bertaggia, E., . . . Merlini, L. (2010). Autophagy is defective in collagen VI muscular dystrophies, and its reactivation rescues myofiber degeneration. *Nature medicine, 16*(11), 1313-1320.

Hall-Craggs, E. (1972). The significance of longitudinal fibre division in skeletal muscle. *Journal of the neurological sciences, 15*(1), 27-33.

Hall, Z. W., & Ralston, E. (1989). Nuclear domains in muscle cells. *Cell, 59*(5), 771-772.

Hansen, E. H. (2009). Effects of SMPX on skeletal muscle in adult mice.

Hartgens, F., & Kuipers, H. (2004). Effects of androgenic-anabolic steroids in athletes. *Sports Medicine, 34*(8), 513-554.

Hawke, T. J., & Garry, D. J. (2001). Myogenic satellite cells: physiology to molecular biology. *Journal of applied physiology, 91*(2), 534-551.

Ho, K. W., Roy, R., Tweedle, C., Heusner, W., Van Huss, W., & Carrow, R. (1980). Skeletal muscle fiber splitting with weight-lifting exercise in rats. *American Journal of Anatomy, 157*(4), 433-440.

Holly, R., Barnett, J., Ashmore, C., Taylor, R., & Mole, P. (1980). Stretch-induced growth in chicken wing muscles: a new model of stretch hypertrophy. *American Journal of Physiology-Cell Physiology, 238*(1), C62-C71.

Jones, G., Gittins, M., & Hardy, L. (2009). Creating an environment where high performance is inevitable and sustainable: The high performance environment model. *Annual Review of High Performance Coaching And Consulting, 1*(13), 94149.

Kadi, F., Schjerling, P., Andersen, L. L., Charifi, N., Madsen, J. L., Christensen, L. R., & Andersen, J. L. (2004). The effects of heavy resistance training and detraining on satellite cells in human skeletal muscles. *The Journal of physiology, 558*(3), 1005-1012.

Kelley, G. (1996). Mechanical overload and skeletal muscle fiber hyperplasia: a meta-analysis. *Journal of applied physiology, 81*(4), 1584-1588.

Lampe, A., & Bushby, K. (2005). Collagen VI related muscle disorders. *Journal of medical genetics, 42*(9), 673-685.

Lapidos, K. A., Kakkar, R., & McNally, E. M. (2004). The dystrophin glycoprotein complex signaling strength and integrity for the sarcolemma. *Circulation research, 94*(8), 1023-1031.

Larsson, L., & Tesch, P. A. (1986). Motor unit fibre density in extremely hypertrophied skeletal muscles in man. *European journal of applied physiology and occupational physiology, 55*(2), 130-136.

Lu, Q., Bou-Gharios, G., & Partridge, T. (2003). Non-viral gene delivery in skeletal muscle: a protein factory. *Gene therapy, 10*(2), 131-142.

MacDougall, J., Sale, D., Alway, S., & Sutton, J. (1984). Muscle fiber number in biceps brachii in bodybuilders and control subjects. *Journal of applied physiology, 57*(5), 1399-1403.

MacDougall, J., Sale, D., Elder, G., & Sutton, J. (1982). Muscle ultrastructural characteristics of elite powerlifters and bodybuilders. *European journal of applied physiology and occupational physiology, 48*(1), 117-126.

Maier, A. (1997). Development and regeneration of muscle spindles in mammals and birds. *The International journal of developmental biology, 41*(1), 1-17.

Mathiesen, I. (1999). Electropermeabilization of skeletal muscle enhances gene transfer in vivo. *Gene therapy, 6*(4), 508-514.

McCall, G., Byrnes, W., Dickinson, A., Pattany, P., & Fleck, S. (1996). Muscle fiber hypertrophy, hyperplasia, and capillary density in college men after resistance training. *Journal of applied physiology, 81*(5), 2004-2012.

Morrison, J. I., Lööf, S., He, P., & Simon, A. (2006). Salamander limb regeneration involves the activation of a multipotent skeletal muscle satellite cell population. *The Journal of Cell Biology, 172*(3), 433-440. doi: 10.1083/jcb.200509011

Pavlath, G. K., Rich, K., Webster, S. G., & Blau, H. M. (1989). Localization of muscle gene products in nuclear domains. *Nature, 337*(6207), 570-573.

Priester, C., Morton, L. C., Kinsey, S. T., Watanabe, W. O., & Dillaman, R. M. (2011). Growth patterns and nuclear distribution in white muscle fibers from black sea bass, Centropristis striata: evidence for the influence of diffusion. *The journal of experimental biology, 214*(8), 1230-1239.

Rennie, M. J., Wackerhage, H., Spangenburg, E. E., & Booth, F. W. (2004). Control of the size of the human muscle mass. *Annu. Rev. Physiol., 66*, 799-828.

Schmalbruch, H. (1976). The morphology of regeneration of skeletal muscles in the rat. *Tissue and Cell, 8*(4), 673-692.

Shenkman, B., Turtikova, O., Nemirovskaya, T., & Grigoriev, A. (2010). Skeletal muscle activity and the fate of myonuclei. *Acta naturae, 2*(2), 59.

Singh, K., Cassano, M., Planet, E., Sebastian, S., Jang, S. M., Sohi, G., . . . Dilworth, F. J. (2015). A KAP1 phosphorylation switch controls MyoD function during skeletal muscle differentiation. *Genes & development, 29*(5), 513-525.

Sinha-Hikim, I., Roth, S. M., Lee, M. I., & Bhasin, S. (2003). Testosterone-induced muscle hypertrophy is associated with an increase in satellite cell number in healthy, young men. *American Journal of Physiology-Endocrinology And Metabolism, 285*(1), E197-E205.

Sjostrom, M., Lexell, J., Eriksson, A., & Taylor, C. (1991). Evidence of fibre hyperplasia in human skeletal muscles from healthy young men? A left-right comparison of the

fibre number in whole anterior tibialis muscles. *European journal of applied physiology and occupational physiology, 62*(5), 301-304.

Sola, O., Christensen, D., & Martin, A. (1973). Hypertrophy and hyperplasia of adult chicken anterior latissimus dorsi muscles following stretch with and without denervation. *Experimental neurology, 41*(1), 76-100.

Somiari, S., Glasspool-Malone, J., Drabick, J. J., Gilbert, R. A., Heller, R., Jaroszeski, M. J., & Malone, R. W. (2000). Theory and in vivo application of electroporative gene delivery. *Molecular Therapy, 2*(3), 178-187.

Tamaki, T., Uchiyama, S., & Nakano, S. (1992). A weight-lifting exercise model for inducing hypertrophy in the hindlimb muscles of rats. *Medicine and Science in Sports and Exercise, 24*(8), 881-886.

Tesch, P. (1988). Skeletal muscle adaptations consequent to long-term heavy resistance exercise. *Medicine and Science in Sports and Exercise, 20*(5 Suppl), S132.

Tipton, K., & Wolfe, R. R. (1998). Exercise-induced changes in protein metabolism. *Acta physiologica Scandinavica, 162*(3), 377-387.

Urban, R. J., Bodenburg, Y. H., Gilkison, C., Foxworth, J., Coggan, A. R., Wolfe, R. R., & Ferrando, A. (1995). Testosterone administration to elderly men increases skeletal muscle strength and protein synthesis. *American Journal of Physiology-Endocrinology And Metabolism, 269*(5), E820-E826.

Vaughan, H. S., & Goldspink, G. (1979). Fibre number and fibre size in a surgically overloaded muscle. *Journal of anatomy, 129*(Pt 2), 293.

Zammit, P. S. (2008). All muscle satellite cells are equal, but are some more equal than others? *Journal of Cell Science, 121*(18), 2975-2982.

Zammit, P. S., Partridge, T. A., & Yablonka-Reuveni, Z. (2006). The skeletal muscle satellite cell: the stem cell that came in from the cold. *Journal of Histochemistry & Cytochemistry, 54*(11), 1177-1191.

Zhao, P., & Hoffman, E. P. (2004). Embryonic myogenesis pathways in muscle regeneration. *Developmental Dynamics, 229*(2), 380-392.

6 Appendix

6.1 List of abbreviations

ATP	Adenosine triphosphate
Akt	Protein kinase B
ALD	Anterior lattisimus dorsi
BSA	Bovine serum albumin
CSA	Cross sectional area
DMD	Dystrophin Glycoprotein Complex
EDL	Extensor digitorum longus
FCR	Flexor carpi radialis
IGF-1	Insulin growth factor 1
MND	Myonuclear domain
mTOR	Mammalian target of rapamycin
MyoD	Myogenic differentiation 1
O2	Diatomic Oxygen
PBS	Phosphate buffer solution
PFA	Paraformaldehyde
PI3K	Phospoinositide 3-kinase
PSO	Progressive stretch overload
SEM	Standard error of mean
TA	*Tibialis anterior*
ZRF	Zoletil forte

6.2 Buffers and solutions

6.2.1 10X PBS (phosphate buffered saline) solution

Solution:	Amount:
NaCl	80.0 g
KCl	2.0 g
Na2HPO4 × 2H2O	14.4g
KH4PO4	2.0g

- Dissolve salts in 800 ml of dH2O
- Adjust volume to 1.1 l, and then adjust pH to 6.8

6.2.2 Hoechst solution

Dilute hoechst (33258, Sigma) in PBS to a final solution of 1µg/ml

Solution:	Amount:
Hoechst	0.4mg
Phosphate buffer solution	400ml

6.2.3 ZRF cocktail solution

Solution:	Amount:
Zoletil Forte 250 mg/ml	5,72 ml
Narcorxyl/Rompun 20 mg/ml	1,72 ml
Fentanyl 50mg/ml	4,00 ml
Sterile isotonic saltwater	8,00 ml

6.2.4 Permeabilization buffer

Solution:	Amount:
Glycine	50 mM
BSA	0.25%
Saponin	0.04%
PBS	0.01M

6.2.5 DNA electroporation solutions

Solution	Amount:
mCherry inserted into (pECFP-Nuc,Clontech loboratories inc)	25 µl
Myrpalm inserted into (pCDNA3, Invitrogen)	25 µl
4 M NaCl	8 µl
dH2O	142 µl

6.3 Histochemistry

6.3.1 Staining for laminin

• Remove sections from -80° freezer and let the sections thaw for 30 min before removing the surrounding foil.

• Apply anti laminin primary antibody produced in rabbit (L-9393, Sigma) in a 1:100 dilution in 1% BSA in PBS. Incubate at 4°C overnight.

• Wash sections 3 × 5 min in 1× PBS (pH 7.2)

• Apply anti-rabbit IgG FITC-conjugated secondary antibody (F9887, Sigma) on primary antibodies in a 1:200 dilution in 1% BSA in PBS. Incubate in room temperature for 1 hour in a dark moist chamber

• Wash sections 3 × 5 min in 1× PBS (pH 7.2)

		Concentrations:	Incubation:
Primary antibody	L9393	1:100	Overnight, 4°C
Secondary antibody	F9887	1:200	1 hour RT

6.3.2 Staining for collagen

• Remove sections from -80° freezer and let the sections thaw for 30 min before removing the surrounding foil.

• Apply anti collagen primary antibody produced in rabbit (ab-19808) in a 1:100 dilution in 1% BSA in PBS. Incubate at 4°C overnight.

• Wash sections 3 × 5 min in 1× PBS (pH 7.2)

• Apply anti-rabbit Alexa 448-conjugated secondary antibody (Z25302, Life technologies) on primary antibodies in a 1:200 dilution in 1% BSA in PBS. Incubate at 4°C overnight.

• Wash sections 3 × 5 min in 1× PBS (pH 7.2)

		Concentrations:	Incubation:
Primary antibody	ab-19808	1:100	Overnight, 4°C
Secondary antibody	Z25302	1:200	Overnight, 4°C

6.3.3 Staining for dystrophin

• Remove sections from -80° freezer and let the sections thaw for 30 min before removing the surrounding foil.

• Apply anti dystrophin primary antibody produced in mouse (D8168, Sigma) in a 1:200 dilution in 1% BSA in PBS. Incubate at 4°C overnight.

• Wash sections 3 × 5 min in 1× PBS (pH 7.2)

• Apply anti-mouse TritC-conjugated secondary antibody (T5393, Sigma) on primary antibodies in a 1:200 dilution in 1% BSA in PBS. Incubate at 4°C overnight.

• Wash sections 3 × 5 min in 1× PBS (pH 7.2)

		Concentrations:	Incubation:
Primary antibody	D8168	1:200	Overnight, 4°C
Secondary antibody	T5393	1:200	Overnight, 4°C

6.3.3 Staining for phalloidin

• Remove teased fiber slides from -80° freezer and let the sections thaw for 30 min before removing the surrounding foil.

• Dilute 5µL methanolic stock solution (A12381) into 200 µL PBS for each coverslip to be stained.

• Apply 200 µL probe/PBS solution (or as much is needed to cover all the fiber), and place in incubation chamber at 32°C for 3 hours

• Wash sections 3 × 5 min in 1× PBS (pH 7.2)

• Cover slides in hoechst solution and image with microscope.

		Concentrations:	Incubation:
F-actin probe	A12381	1:200	3 hours, 32°C